Journal of Korean Institute of surface Engineering
Vol. 29, No. 6, Dec., 1996

INVESTIGATIONS OF OXIDATIONS OF SnO_X AND ITS CHANGES OF THE PROPERTIES PREPARED BDEPOSITIONY REACTIVE ION-ASSISTED

J. S. Cho, W. K. Choi, Y. T. Kim, H. J. Jung and S. K. Koh

Division of Ceramics, Korea Institute and Technology, Cheongryang P. O. Box 131 Seoul 130-650, Korea

ABSTRACT

Undoped SnO_X thin films were deposited on Si(100) substrate by using reactive ioassisted deposition technique (R-IAD). In order to investigate the effect of initial oxygen content and heat treatment on the oxidation state and crystalline structure of tin oxide films, SnO_X thin films were post-annealed at 400~600℃ for 1 hr. in a vacuum $\sim 5 \times 10^{-3}$ Torr or were directly deposited on the substrate of 400℃ and the relative arrival ration (Γ) of oxygen ion to Sn metal varied from 0.025 to 0.1, i.e., average impinging energy (E_a) form 25 to 100 eV/atom. As E_a increased, the composition ratio of N_0/N_{Sn} changed from 1.25 to 1.93 in post-annealing, treatment and 1.21 to 1.87 in in-situ substrate heating. In case of post-annealing, the oxidation from SnO to SnO_2 was closely related to initial oxygen contents and post-annealing temperature, and the perfect oxidation of SnO_2 in the film was obtained at higher than E_a=75 eV/atom and 600 ℃. The temperature for perfect oxidation of SnO_2 was reduced as low as 400℃ through in-situ substrate heating. The variation of the chemical state of SnO_X thin films with changing E_a's and heating method were also observed by Auger electron spectroscopy.

INTRODUCTION

SnO_2 thin films have wide applications such as transparent electrodes, optoelectronic devices, high photothermal conversion of SnO_2/Si solarcell, and inflammable gas sensor devlices[1~4]. Various techniques, i.e., spray pyrolysis[5], chemical vapor deposition (CVD)[6,7], sol-gel method[8], reactive evaporation[9], and sputtering[10,11] have been employed to obtain SnO_2 thin films. In case of reactive evaporation or sputtering using SnO_2 bulk material as evaporant or sputtering target, the SnO_2 molecules generally decompose in gaseous state and mainly SnO condenses on the substrate. Hence, tin oxide thin films could be perfectly obtained by either applying in-situ substrate heating with flowing oxygen gas during the deposition or through a post annealing procedure in oxygen ambient or air at high temperature over 600℃[9~11]. Such a high post annealing temperature would much affect stoichiometry and surface morphology of deposited tin oxide films, hence it is not suitable for practical fabrication.

Many thin films including dielectric oxides, fluorides, transparent conductors, and nitrides have been prepared by an ion-assist deposition (IAD)[12,13] but there have been few reports on deposition and properties of SnO_2

films. The ion-assisted deposition technique influences a number of film properties including adhesion, morphology, stoichiometry, stress, and packing density by delivering different energy or momentum to depositing materials and/or substrate[14-17]. In particular, additional activation energy can be added to the growing film if it is bombarded with energetic ions during deposition and in consequence it is expected to lower the substrate temperature for thin film formation.

In this work, we fabricate undoped tin oxide films with different oxygen contents which were treated by post-annealing and were grown on heated substrate by using reactive ion-assisted deposistion and investigate the oxidation state of the deposited tin oxide films. Also we examine the effect of the initial composition and heat treatment on the final crystalline structure of the films.

EXPERIMENTAL PROCEDURE

Undoped SnO_x thin films with about 1000 Å thickness were grown on si (100) substrate by a reactive ion-beam assisted deposition(R-IAD). Neutral Sn metal was evaporated by using a partially ionized beam (PIB) source at a rate of 0.5 Å/sec and concurrently oxygen ions were assisted by using 5cm gridded cold hollow cathode ion gun. Oxygen ions were accelerated at constant ion-beam supply potential of 500 V and an average impinging energy (E_a) delivered to deposited Sn particle, was changed from 25 to 100 eV/atom by the variation of discharge current, i.e., relative arrival ration (Γ) of ion to Sn particle. Since the oxygen ion-beam current extracted from the source is normally lower at the sample position apart from 45cm from the source than that ahead of ion source optic grid, the current density at the sample surface was calculated from the reading ion-beam current density monitored by a Faraday cup placed at the sample aside. The base vacuum pressure before deposition was 8×10^{-6} Torr and deposition was performed at 2×10^{-4} Torr with oxygenion irradiation. As-deposited tin oxide films were annealed at 400～600℃ for 1hr in the vacuum chamber evacuated to 50 $\times10^{-3}$ Torr without flowing any gases. In case of in-situ heating, the substrate was heated at 400℃ during the deposition. Other experimental conditions were described in detail elsewhere[16,17].

RESULTS AND DISCUSSION

Post-annealing of tin oxide films at varionus temperatures

a. Crystalline structure studies

The crystalline structures of as-deposited tin oxide films appear amorphous by XRD studies (not shown here). In the following contents, the post-annealed films are denoted as "A25" and the in-situ substrate heated films as "S25" respectively, where suffix digit represents average impining energy. As shown in Fig. 1(a), tin oxide films annealed at 400 ℃ represent the XRD peaks related to polycrystalline SnO phases upto E_a=50 eV/atom (a40). The film A25 (Fig. 1(a)) shows many XRD peaks of SnO(101), SnO(002), SnO (112), and SnO(211). for the film A50, the intensity iof XRD peaks for SnO(002) and SnO(112) decrease and the peak of SnO (200) arises. In the XRD patterns of the films deposited at higher than E_a = 50 eV/

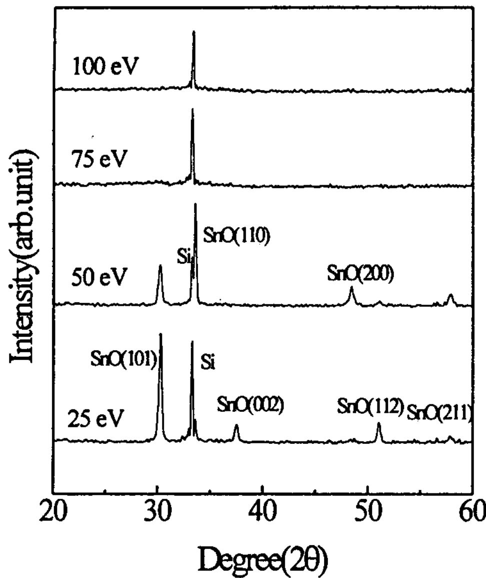

Fig. 1(a) The XRD patterns of the tin oxide films annealed at 400℃ in vacuum(5×10^{-3} Torr) for 1 hr.

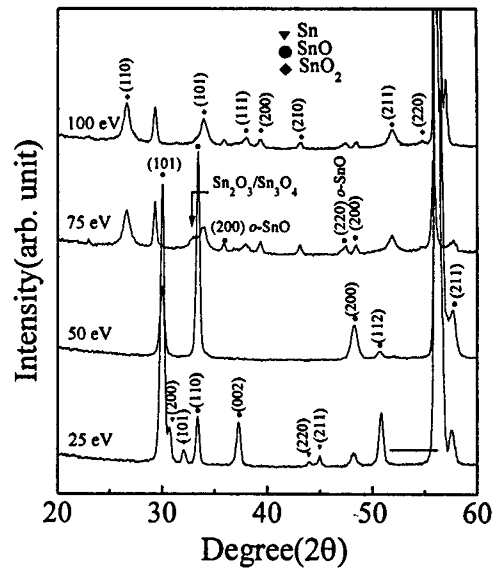

Fig. 1(b) GXRD patterns of the tin oxide films annealed at 500℃ in vacuum(5×10^{-3} Torr) for 1 h.

atom, no peak can be detected and thus those films still have amorphous structures like the as-dep-osited films. In the GXRD patterns of the tin oxide films annealed at 500℃ (Fig. 1 (b)), the similar results are observed except the peaks related to metallic β-Sn in the film A25. The appearance of metallic β-Sn peaks results from the metallic tin segregation in films due to the increase of the annealing temperature and this result was already identified by Geurts. et al. and Klushin et al.[18,19] But no peak of metallic β-Sn in observed in the film A50 (Fig. 1 (b)). It cal be explained that the oxygen content of the film A50 is higher than that of the film A25 and thus the film A50 is entirely oxidized into SnO without tin segregation. For the film A75, it is shown that the XRD patterns of polycrystalline SnO_2 including α-SnO and o-SnO (orthorhombic) and intermediate Sn_2O_3/Sn_3O_4. The peaks of intermediate Sn_2O_3/Sn_3O_4 dis appear in the film A100 and the mixed phase of SnO and SnO_2 exist in the film. From the result of Fig. 1(b), the films annealed at 500℃ are not perfectly oxidized to SnO_2 and the annealing temperature is not so sufficient as to form SnO_2. Geurts et al.[18] reported that the film deposited by evaporation of SnO_2 powder is perfectly oxidized after post-annealing at higher than 600℃ in O_2 atmosphere. In present work, the only XRD pattern of SnO_2 phase is observed in the film A100 annealed at 600℃. Therefore it can be said that the film is perfectly oxidized to SnO_2. This result is well consistent with the previous results[18,19].

Figure 2 shows the SEM micrographs of the surface for the films annealed at 500℃. As shown in Fig. 2(a), the film A25 is composed of the rod-shaped grains which have a length of 600 Å and a width of about 1000 Å (aspect ration 6 : 1). The SEM micrograph of the film A50 indicates that the aspect ratio

of the rod-shaped grain is reduced (not shown here). From the GXRD studies, this result may be due to the change of the crystalline structure in the film. The SEM micrograph of the film A100 shows that the granular grains are uniformly distributed and the average size of the granular grains is about 300Å. As can be seen in Fig. (b), the appearance of the granular grains is due to the formation of SnO_2 phase.

b. Composition and chemical shifts studies.

In order to investigate the composition and the chemical state of the films annealed at 500℃ with E_a's, Auger electron spectroscopy (AES) was performed. The Auger spectra of pure tin metal and SnO_2 powder are used for standard to evaluate the composistion and chemical state of the films. From the derivative Auger spectra, the atomic ratios of N_o/N_{sn} in the films are calculated by using a differential peak-to-peak height of O $KL_{2,3}$ $L_{2,3}$ transition and Sn M_4 $N_{4,5}$ $N_{4,5}$ transition lines in the unknown corrected by intensity computed for standard SnO_2 powder assumed stoichiometric[20]. The calculated N_o/N_{Sn} ratios of the films and the chemical shift of the characteristic Sn M_4 $N_{4,5}$ $N_{4,5}$ Auger transition line compared to Sn metal are listed in Table 1. As shown in Table 1, N_o/N_{Sn} increases from 1.14 to 1.91 as E_a increases and all characteristic Sn MNN transition lines shift toward lower kinetic energy. This result is to be expected from the elementary bonding consideration. The electron charge transfer upon bonding is from the tin cation to the more electronegative oxygen atom. The subsequent increase in the effective nuclear charge of tin causes the inner shell binding energy level to shift toward a higher binding energy. The MNN transition of pure tin Sn metal shifts from 437.4 eV to 433.2~433.6 eV for the Sn-SnO mixed phase film(A25) and pure SnO film(A50). This peak moved further to lower kinetic energy of 432.6 eV in case of the film A100. These results of chemical shift with changing the phase agree with

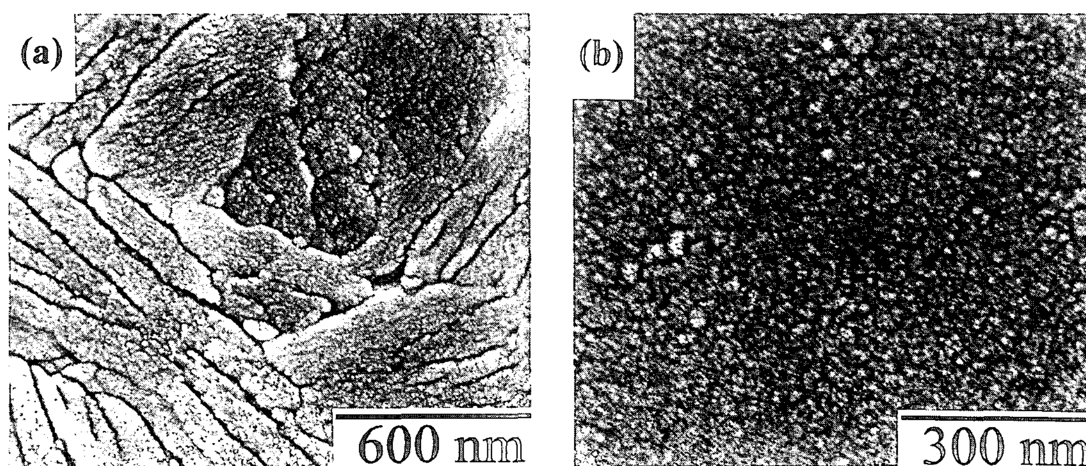

Fig. 2 The SEM micrographs the tin oxide films annealed at 500℃ : (a) A25 and (b) A100

Table 1. Observed Auger electron energies(E_{obs}) for $N_4N_{4,5}N_{4,5}$ transition in pure tin, post-annealed tin oxide films, *in-situ* heated tin oxide films, pure tin oxide powder and calculated N_o/N_{Sn} ratio in the films

Species	Post-annealed tin oxide films		*In-situ* heated tin oxide films	
	E_{obs}(eV)	N_o/N_{Sn}	E_{obs}(eV)	N_o/N_{Sn}
Sn metal	437.4	0.00	437.4	0.00
E_a= 25eV/atom	433.6	1.25	433.9	1.21
E_a= 50eV/atom	433.2	1.44	433.7	1.23
E_a= 75eV/atom	432.8	1.80	432.6	1.63
E_a=100eV/atom	432.6	1.91	432.4	1.87
SnO_2 powder	432.4	2.00	432.4	2.00

the previous reuslt[21] and the change of N_o/N_{Sn} ratios and chemical shift for the films is well consistent with the results of the GXRD studies and the SEM micrographs.

In-situ substrate heated tin oxide films

a. Crystalline structure

Figure 3 shows the GXRD patterns of the films deposited at 400℃ substrate temperature at various average impinging energies (E_a's). The film deposited at E_a=25 eV/atom (S25) contains polycrystalline SnO and β-Sn. In case of the film S50, the intensity of the peaks for β-Sn become small and that of the peak related to the SnO(002) increase. This means that the film is crystallized into tetragonal SnO. It is worth while to note that the peaks of the SnO and β-Sn phases are vanished in the film S75 and the peak corresponding the SnO_2(101) phase newly arises. The line width of the SnO(002) broadens and the position of the peak shifts to lower diffraction angle in the film S75. Such broadening and the shift of the peak indicate that the film has a mechanical strain due to the coexistence of SnO and SnO_2 phases[12]. For the film S100, it is observed that the film has the SnO_2 phases corresponding to (110), (101) and (211) planes and thus it can be believed that the film is perfectly ozidized into SnO_2. The GXRD patterns of the films deposited at higher than 400℃ are not different from those of the films deposited at 400℃. It can be summarized that the temperature of the SnO_2 formation can be reduced at lower temperature as much as 400℃.

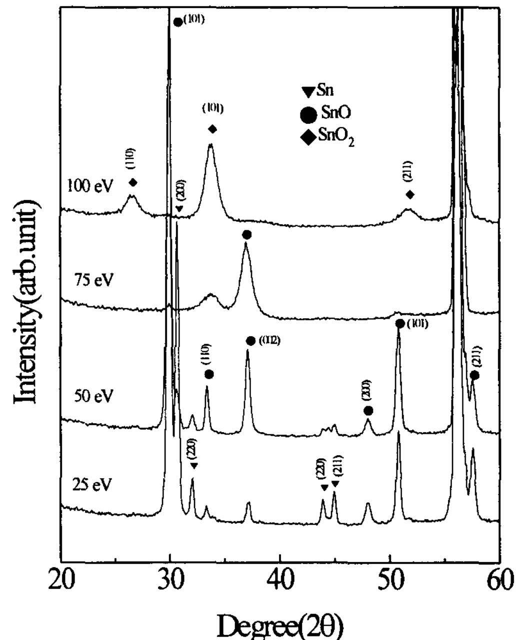

Fig. 3. The GXRD patterns of the tin oxide films deposited at 400℃ substrate temperature.

Figure 4 is the SEM micrographs of the films deposited at various E_a's. The crystall-

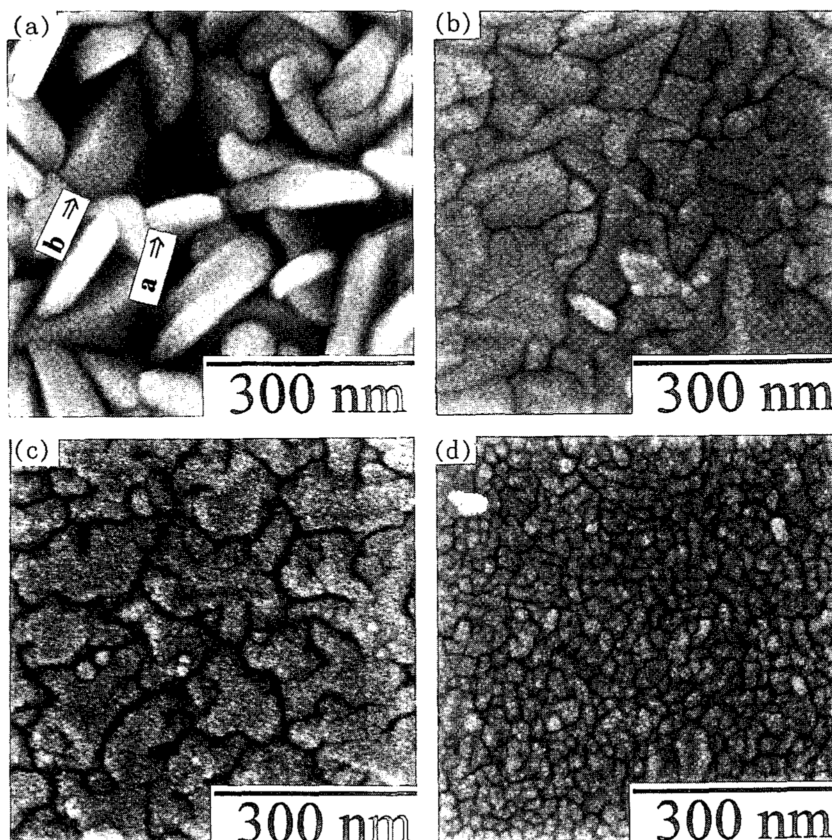

Fig. 4. The SEm micrographs the tin oxide films deposited at 400℃ substrate temperature (a) S25, (b) S50, (c) S75 and (d) S100

ites of the film S25 (Fig. 4(a) are composed of two kinds of grains: one is that of β-Sn (denoted as A) and the otehr is that of SnO(B). As shown in Fig. 4(b), the crystallites of the film S50 mainly consist of the SnO and this result have a good agreement with the GXRD pattern in Fig. 4. The different shapes of the crystallites show up in the film S75 (Fig. 4(c)) and this is closely related to the mixed SnO and SnO_2 phases compared to the GXRD pattern. The film S100 has the granular crystallites with a size of 300～500Å and these crystallites are distributed uniformly in the film. Comparing with the SEM photograph of post-annealed film (Fig. 2(b)) and the GXRD pattern (Fig. 3), it is concluded that the film S100 is perfectly oxidized into SnO_2.

b. Composition and chemical shifts studies

The calculated N_o/N_{Sn} ratios of the deposited flims with various E_a's and the chemical shift of the characteristic Sn $M_4N_{4,5}N_{4,5}$ Auger transition line compared to Sn metal are also listed in Table 1. As shown in Table 1, N_o/N_{Sn} increases from 1.21 to 1.87 as E_a increase and the all characteristic Sn MNN transition lines shift toward lower kinetic energy. These trends are nearly similar to those of the post-annealed films.

CONCLUSIONS

The composition of undoped nostoichio-metric SnO_x thin films was quasi continuously controlled by using R-IAD. After post-annealing in a vacuum condition, the crystallinity of the films were dependent of the initial composition of the film and the post-annealing temperature. The perfect oxidation into SnO_2 was performed at 600℃ in the post-annealing process. In in-si-tu substrate heating, the crystallinity of the film was also affected by the initial composition and the film was perfectly oxidized into SnO_2 at 400℃ substrate temperature. In in-situ heated the films, the intermediate phase Sn_2O_3/Sn_3O_4 which exist in the post-annealing was not found. In consequently, the temperature of the SnO_2 formation can be reduced at lower temperature as much as 400℃ in in-situ substrate heating than post-annealing

REFERENCES

1. K. L. Chopra, S. Major and D. K. Pandya, Thin Solid Films **102** 1(1983).
2. V. K. Jin and A. P. Kulshreshtha, Sol. Energy Mater. **4** 151(1981).
3. J. Sanz Maudes and T. Rodriguz, Thin Solid Films **69** 183(1980).
4. K. D. Schierbaum, U. Weimar and W. Gael, Sensors and Actuators **B7** 709 (1992).
5. G. Martinelli, L. Szepessy, J. F. Bresse, M. Perotin and R. Stuck, Mater. Res. Bull. **14** 109 (1979).
6. K. H. Kim and T. park, J. Kor. Phys. Soc. **18** 124 (1985).
7. D. Liu, Q. Wang, H. L. M. Chang and H. Chen, J. Mater. Res. **10** 1516 (1995).
8. S. S. Park and J. D. Mackenzie, Thin Solid Films **258** 268 (1995).
9. M. H. Mashusudhana reddy, S. R. Jawalekar and A. N. Chandorkar, Thin Solid Films **169**, 117 (1989).
10. M. R. Soares, P. H. Dionisio, I. J. R. Baumvol and W. H. Schreiner, Thin Solid Films **214** 6 (1992).
11. B. Stjerna, E. Olsson and C. G. Granqvist, J. Appl. Phys. **76** 3797 (1994).
12. P. J. Martin and R. P. Netterfield, Thin Solid Films **137** 207 (1987).
13. J. A. Dobrowolski, F. C. Ho and A. Waldorf, Appl. Opt. **26** 5204 (1987).
14. M. Satou and F. Fujimoto, Jap. J. Appl. Phys. **22** 171 (1983).
15. J. J. Cuomo and S. M. Rossnage, Hand book of Ion Beam Processing Technology (Noyes Publications, New Jersey, 1989) p. 387.
16. W. K. Choi, H-J. Jung and S. K. Koh, J. Vac. Sci. Technol. **A14** 359 (1996).
17. W. K. Choi, J. S. Cho S. K. Song, H-J. Jung and S. K. Koh Jap. J. Appl. Phys. (inpress).
18. J. Geurts, W. Richter and F. J. Schmitte, Thin Solid Films **121**. 217 (1984).
19. D. N. Klushin, O. V. Nadinskaya and K. G. Bogatin, Zh. Prikle. Khim. **31**, 273 (1959).
20. P. J. Martin and R. P. Netterfield, Thin Solid films **137** 207 (1986).
21. S. K. Sen, S. Sen and C. L. Bauer, Thin Solid Films **82** 157 (1981).